Tellus (1987), *39A*, 138–151

Teleconnections of rainfall anomalies and of the Southern Oscillation over the entire tropics and their seasonal dependence

By HARTMUT BEHREND, *Max-Planck-Institut für Meteorologie, Bundesstrasse 55 D-2000 Hamburg FRG*

(Manuscript received July 31, 1985; in final form June 19, 1986)

ABSTRACT

The teleconnections between rainfall anomalies of selected areas within the tropics to each other are investigated with respect to their seasonal dependence, employing a cross correlation analysis technique. They are related to the Southern Oscillation. The magnitude and phase of these rainfall anomalies are computed for a typical El Niño event using a so-called composite analysis. Rainfall anomalies persist for almost an entire year over the islands of the equatorial Central Pacific, whereas over most areas in and around the tropical Indian and Pacific Ocean, they only tend to persist for a season or two. Seasons during which rainfall anomalies are most persistent (in a particular region) are also seasons, during which teleconnections between rainfall anomalies of these regions to each other are strongest. The Southern Oscillation is negative-correlated with the majority of the rainfall anomalies except for those from India, Indonesia, Hawaii and the Northcoast of Venezuela. The rainfall anomalies calculated for a typical El Niño event fit into this general scheme of teleconnections.

1. Introduction

The Southern Oscillation (SO), which has been comprehensively reviewed by Berlage (1957), Troup (1965) and Julian and Chervin (1978) represents the variation of pressure difference between the Indonesian low and the South Pacific subtropical high. It is intimately connected with the El Niño event occurring along the Peruvian coast and along the equatorial Central Pacific Ocean, because during an El Niño, the positive sea surface temperature (SST) anomalies can only develop when the tradewinds over the Pacific are weak; hence a weak pressure gradient between Indonesia and the South Pacific constitutes a prerequisite (Bjerknes, 1969).

The SO is to a large extent governed by the thermodynamically direct tropical circulation cells which are driven by the differences in atmospheric latent heating. The most important source region of atmospheric latent heating is located over Indonesia (Ramage, 1968). Latent heating is positive-correlated with the total amounts of rainfall because latent heat is released when water condenses and precipitates. It is therefore assumed that rainfall anomalies represent variations in latent heating.

The primary region of tropical rainfall is the Inner Tropical Convergence Zone (ITCZ), which is fed by moisture being carried by the trades. Hence, the strength and convergence of the trades are of great importance when considering teleconnections of tropical rainfall anomalies. For this reason, the trade winds as well as SST anomalies have attracted more attention than rainfall anomalies in order to explain the El Niño phenomenon (Rasmussen and Carpenter, 1982).

The SO/El Niño event is explained by atmospheric-oceanic feedback mechanisms of which the most important ones are: (a) the positive correlation between SST and rainfall anomalies when the trades weaken over the Pacific (Bjerknes, 1969); (b) an equatorial Kelvin wave lowering the thermocline (Wyrtki, 1975); (c) the

enhanced transport of warm water within the Northequatorial Counter Current (Wyrtki, 1973); (d) the propagation of a positive SST anomaly to the west within the Central and Eastern Pacific (Wells, 1979); (e) the merging of the ITCZ and the Southpacific Convergence Zone in the vicinity of the dateline (Trenberth, 1976), causing the Indonesian low to shift its position into that area (Ichiye and Pettersen, 1963).

Based upon correlations between rainfall anomalies within the tropics, several teleconnections have already been discovered. For example, there is a negative correlation between the rainfall anomalies of the stations within the equatorial Pacific and those of the Indonesian southeast monsoon, of the Indian southwest monsoon and of the Southwest Pacific (Nicholls, 1981; Angell, 1981; Donguy and Henin, 1980). The rainfall anomalies between the equatorial Pacific and Sri Lanka are correlated positively with one another (Rasmussen and Carpenter, 1983).

In this paper, rainfall anomalies at stations distributed over the entire tropics are correlated with one another in order to derive a more complete understanding of these teleconnections. The occurrence of teleconnections in association with the SO is also investigated. The seasonal dependence of teleconnections is stressed because of the seasonality characterizing tropical rainfall and the occurrence of the El Niño event. Teleconnections may be existent in space and time, so that in addition to simple correlations, time lags have been included as well. Section 3 presents an autocorrelation analysis exploring the persistence of the rainfall anomalies with respect to their seasonal dependence. Teleconnections are then computed in Section 4. In Section 5, composites of a few selected time series were established in order to show the magnitude of the rainfall anomalies during an average El Niño.

2. Data

Rainfall data used in this paper represent monthly values. The rainfall anomaly of a month is defined by the deviation from the average rainfall amount computed for that particular calendar month over the entire time series. Table 1 lists the stations or area means of the rainfall time series employed in the correlation analysis. Fig. 1 presents the geographical locations of these stations and areas. However, note that most of the time series are based upon data representing area means. Area means were determined when rainfall series of individual stations within a certain area were significantly and positively correlated with each other (verification by the Student-t test). The advantages of using area means are: (a) the amount of data is reduced; (b) small-scale effects exhibited by single rainfall stations and inhomogeneities are averaged out; (c) large-scale variations of convective activity are more likely to be detected than by a single rainfall station which might fail to show this variation of tropical rainfall due to the small-scale character of convective cells.

In addition to rainfall data, the following time series were employed in the cross correlation analysis of Section 4: (a) SO-Index from 1852 until 1973, computed by Wright (1975); (b) SST time series of Christmas Island (1°59′N/157°22′W) from 1951 until 1977, constructed by Weber (Flohn, 1984).

These two time series are also based upon monthly mean values, although monthly means of the SO-index had to be obtained by interpolating from the quarterly means originally given by Wright (1975). Instead of using air pressure as done by Berlage (1957) or pressure differences as done by Quinn and Burt (1972), Wright (1975) performed an empirical orthogonal function analysis of the pressure anomalies of Cape Town, Bombay, Djakarta, Darwin, Adelaide, Apia, Honolulu and Santiago, and defined the SO-index as the amplitude of the first eigenvector. The SO-index was normalized in order to obtain a mean of 0 and a standard deviation of 1.

3. Autocorrelation analysis

Based upon the time series listed in Section 2, an autocorrelation analysis was performed in order to investigate whether rainfall anomalies of a particular area or station would indicate a seasonal variation of persistence. For this analysis, the autocorrelation coefficients between rainfall anomalies of a particular calendar month and those of an arbitrary subsequent month were computed by applying different time lags. A time lag of 1 month means that, e.g. the January

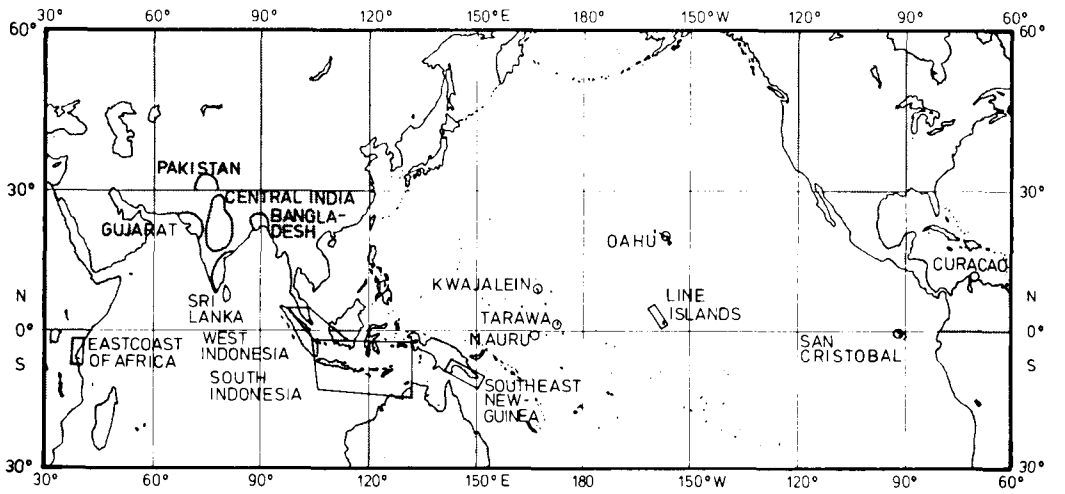

Fig. 1 Geographical position of rainfall series used in the cross-correlation analysis.

anomalies were correlated with the February anomalies in the same year, a time lag of 12 months means these January anomalies were correlated with the January anomalies in the subsequent year. However, it should be noted that the autocorrelation analysis was performed on time series of different length as listed in Table 1.

Fig. 2 summarizes the principal results of the autocorrelation analysis for a number of stations and area means by plotting the calendar months for which autocorrelations of the rainfall anomalies were computed vs the time lag. The length of a bar denotes for how many months a rainfall anomaly occurring in this particular month tends to persist. Autocorrelation coefficients considered in this figure had to be positive and significant at the 90% confidence limit. In addition, the height of the bar was determined by requiring an uninterrupted sequence of positive and significant correlation coefficients.

For each subdiagram, a triangle can be identified in which rainfall anomalies between any 2 months are significant and positive. However, as can be seen, the base of the triangle, or the season during which rainfall anomalies tend to exhibit persistence (time period denoted by the horizontal black bar) may occur during different times of the year and may last from 3 up to 12 months.

The subdiagram of Central India, for instance, indicates that the rainfall anomalies of July (7) are significantly and positive-correlated with those of the following August, September and October (first bar), those of August (8) correlate with those of the following September and October (second bar), and those of September correlate with those of October (third bar). If a rainfall anomaly has occurred in July, it tends to persist during the following months of the southwest monsoon until October. The monsoon break around August, as quite often seen in the total amount of precipitation (Ramage, 1971), is not reflected in the autocorrelation analysis.

In South Indonesia, the persistence of the rainfall anomalies is present during the southeast monsoon (July–November), but is absent during the northwest monsoon. Nicholls (1981) explained this feature as being caused by the existence of a feedback mechanism between wind- and SST anomalies, which is positive during the southeast monsoon, but negative during the rest of the year. The same feature is observed in Southeast New Guinea. Along the equatorial Central Pacific (Nauru, Tarawa, Line Islands), rainfall anomalies are persistent over an entire year, lasting from June until the following April, a result already pointed out by Wright (1979). Interestingly, SST anomalies at Christmas Island as well as the SO-index display the same persis-

Table 1. *Rainfall series of the cross-correlation analysis*

Rainfall series	Time range	Source	Extent (km²)	Amount of station
North Pakistan	1900–1960	Schweizer	60,000	11
Gujarat	1875–1974	Schweizer	150,000	27
Bangla Desh	1900–1960	Schweizer	90,000	9
Central India	1870–1974	Schweizer	450,000	10
Southeast India	1835–1974	Schweizer	200,000	7
Sri Lanka	1875–1975	Raatz	60,000	13
West Indonesia	1879–1970	*	900,000	4
South Indonesia	1879–1970	*	3,300,000	13
Southeast New Guinea	1904–1972	*	500,000	6
Nauru	1892–1972	Fleer		
Tarawa	1926–1980	Taylor, MCD		
Line Islands	1910–1975	Meisner	200,000	3
Oahu	1891–1975	Meisner	5,000	9
San Cristobal	1950–1980	Becker		
Curaçao	1895–1970	Becker		
East coast of Africa	1893–1971	Helbig	200,000	6

Table 1a. *Geographical position of rainfall stations*

Station	Geographical position
Nauru	0°34′S/166°55′E
Tarawa	1°21′N/172°56′E
San Cristobal	1°09′S/89°06′W
Curaçao	12°12′N/68°58′W
Washington Island	4°43′N/160°25′W
Fanning Island	3°55′N/159°23′W
Christmas Island	1°59′N/157°22′W
Canton Island	2°46′S/171°43′W

The extent in the 4th column is the extent of the corresponding region. The sources of the 3rd column are listed in the references. MCD means "Monthly Climatic Data of the World".

tence characteristics (Wright, 1977). The reason for the persistence of the SO-index is still unknown, but it seems to be intimately linked with the onset (around June) and ending (around April) of El Niño in this equatorial region (see section 5). Additionally, the rainfall anomalies are persistent over the East coast of Africa during the second rainy season (September–December); they are also persistent at San Cristobal/Galapagos and at Curaçao off the northcoast of Venezuela during their respective rainy seasons. An interesting feature, seen in most rainfall series, is the occurrence of strong persistence around September, when most teleconnections are strongest as well (see Section 4).

4. Cross correlation analysis

Based upon the time series listed in Section 2, a cross-correlation analysis was performed in order to explore the existence of teleconnections of rainfall anomalies. For this purpose, a cross-correlation matrix of rainfall anomalies was computed for each possible pair of time series. Included in this matrix are the correlation coefficients between the 12 calendar months of

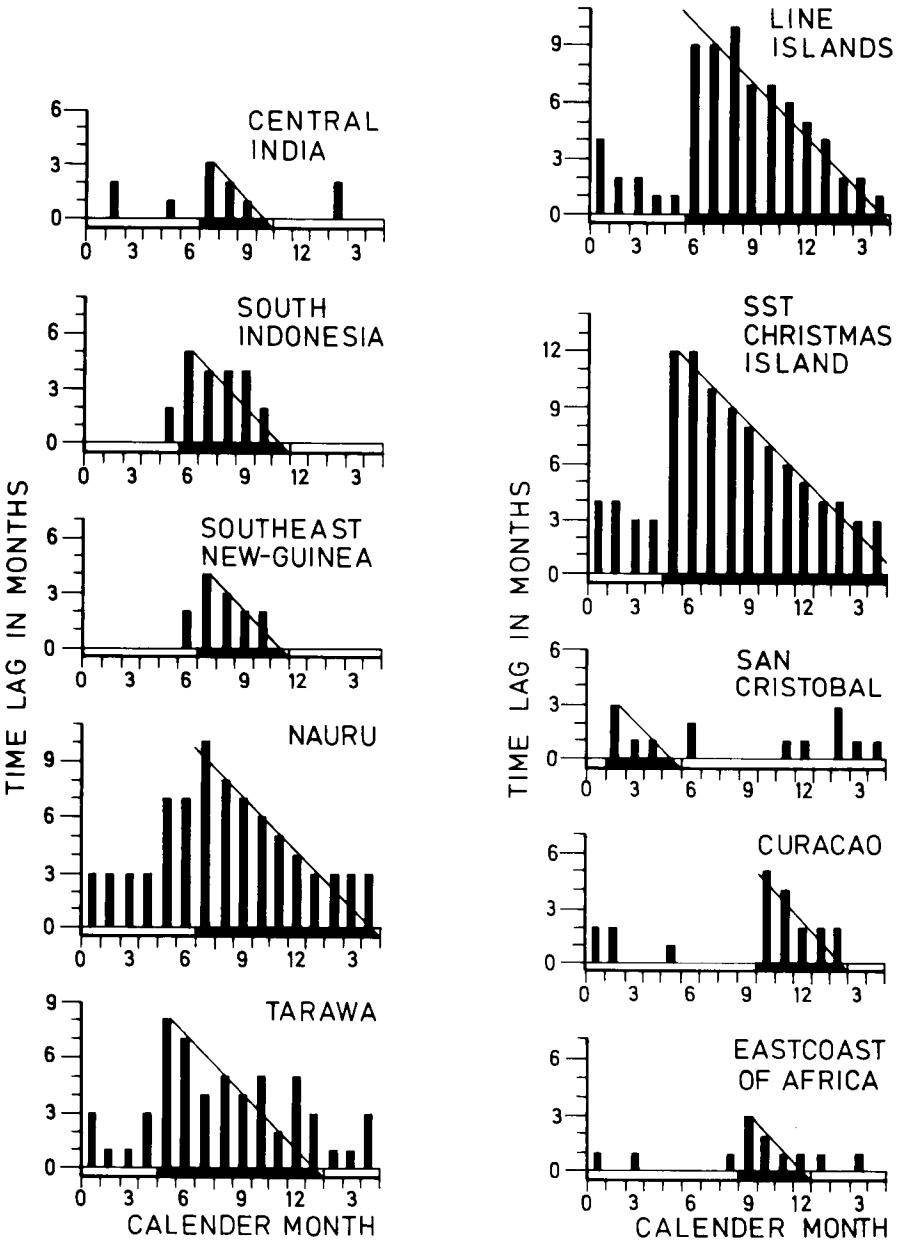

Fig. 2 Results of the autocorrelation analysis.

the primary time series and the months of the secondary series, using time lags varying between −12 and +12 months. Hence, a correlation matrix consists of 12·25 correlation coefficients. A portion of this matrix was called significant when more than 10% of the correlation coefficients were exceeding the 90% confidence limit. This was done in order to avoid misinterpretation due to randomly existing correlation coefficients. In addition, the restriction had to be tightened by

including the influence of persistence, which reduces the number of degrees of freedom. This was done by computing the "equivalent number of persistence" E (Bartels, 1935) defined as

$$E = 1 + 2 \sum_{i=1}^{N} \frac{N-i}{N} \operatorname{accf}(i)$$

where $\operatorname{accf}(i)$ is the autocorrelation coefficient ($-1 \leq \operatorname{accf}(i) \leq 1$) with time lag i, and N is the greatest number of time lags considered, in this case 24. E was calculated for each individual time series, and for a given cross-correlation matrix a mean $\bar{E}$ was calculated. Hence, the number of significant correlation coefficients present in a portion of the matrix had to be reduced by a factor $\bar{E}$ in order to decide whether the portion was significant or not. Portions of significant correlation coefficients represent teleconnections between time series during a distinct period of the year.

Figs. 3, 4 summarize the principal results of the cross-correlation analysis. Displayed are all significant correlations between rainfall anomalies and the SO-index. Time intervals indicated next to the circles are those which were contained within the significant portion of the cross-correlation matrix of that particular rainfall series with the SO-index. That means, for example, that during the period May–April, the SO-index has teleconnections with the January–April period of rainfall anomalies at Oahu/Hawaii. The most significant correlation coefficients occur when the rainfall anomalies of Oahu lag the SO-index by 4 months, denoted by the boxed number 4 along the connection line and by the arrow pointing towards Oahu. The differently marked connection lines indicate the magnitude of the most significant correlation coefficients (see figure caption). Hatched areas are correlated negatively with the SO-index.

The results of Fig. 3 are:

(1) During the Indian southwest monsoon, Central India, Gujarat and North Pakistan have teleconnections with the SO-index which are positive and without a time lag.

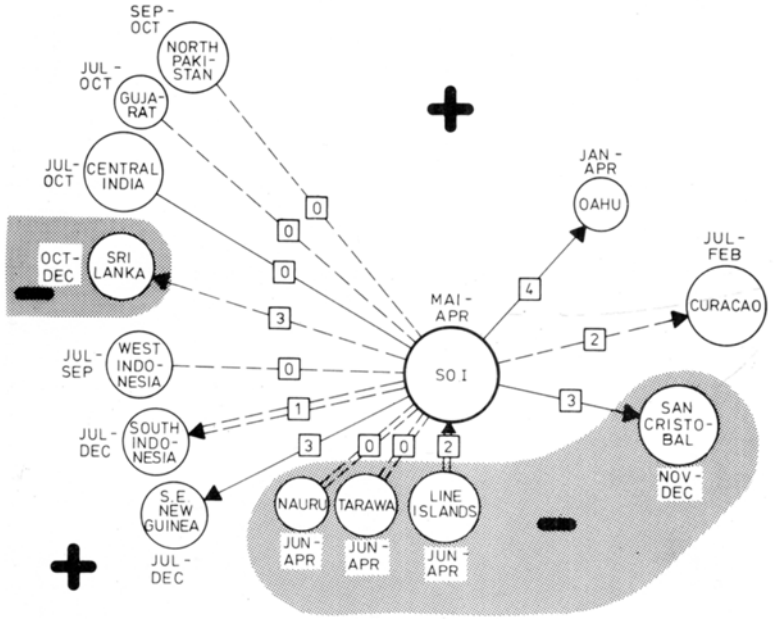

Fig. 3 Teleconnections with the SO-index. (SOI). The connection lines between a time series and the SO-index show the size of the most significant correlation coefficient (ccf):

⟹ ccf ≥ 0·8
= = = ▶ 0·7 ≤ ccf < 0·8
——▶ 0·6 ≤ ccf < 0·7
- - -▶ ccf < 0·6

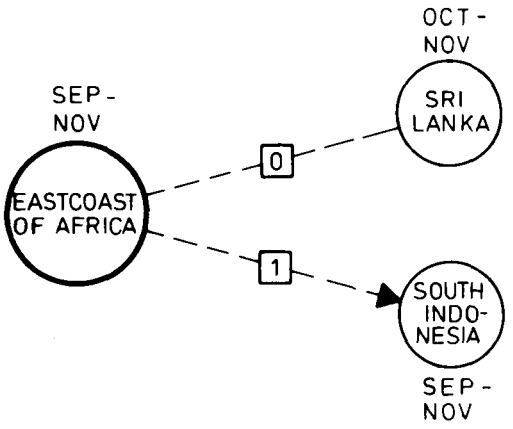

Fig. 4 Teleconnections with the east coast of Africa.

While on the Indian subcontinent the significant correlations end in October, they last until the following April in the time series of the SO-index.

(2) During the second intermonsoonal season, the teleconnections between Sri Lanka and the SO-index are negative, while Sri Lanka lags the SO-index.

(3) During the southeast monsoon over Indonesia, South Indonesia, West Indonesia and Southeast New Guinea show positive teleconnections with the SO-index. Only the teleconnections between Southeast New Guinea and the SO-index have a noticeable time lag of 3 months, where the rainfall anomalies are lagging the SO-index.

(4) During the rainy season at Oahu/Hawaii and Curaçao off the northcoast of Venezuela, the teleconnections with the SO-index are positive, lagging the SO-index by 4, respectively 2 months.

(5) Throughout June until the following April, the simultaneous teleconnections between the SO-index and the islands within the equatorial Central Pacific (Nauru, Tarawa, Line Islands) are negative. Only the rainfall anomalies of the Line Islands lag the SO-index by 2 months.

(6) The rainfall anomalies of the months November until December at San Cristobal lag by 3 months the SO-index during the whole period May until April of the following year, while they are negative.

Fig. 3 represents a scheme of teleconnections which will be retained when exchanging the SO-index with any other station/area mean without changing the time periods indicated next to the station/area mean. It is very important to note that the occurrence of teleconnections is seasonally fixed. The seasons when these teleconnections occur, correspond to the seasons when the rainfall anomalies are also most persistent (see Section 3).

Another scheme of teleconnections has been discovered to exist between the east coast of Africa (during its shorter rainy season) and Sri Lanka (during the second intermonsoonal season) and South Indonesia (during the southeast monsoon) as shown in Fig. 4.

Fig. 3 reproduces the pattern of the Pacific Walker circulation (Bjerknes, 1969), which causes air to subside along the equatorial Pacific at the same time as when atmospheric convergence also includes India and Indonesia but only during the times of the southwest monsoon or southeast monsoon, the season, when these areas are influenced by the circulation of the southern hemisphere.

The scale of the teleconnection scheme displayed in Fig. 3 is almost global in extent with a distance of 20,000 km between San Cristobal and Central India, while it is much smaller for the teleconnection scheme existing over the Indian Ocean displayed in Fig. 4. The latter one is also much weaker and can only be detected during that season when the ITCZ passes over the Eastcoast of Africa and over Sri Lanka while moving southward.

The following overall scheme now becomes evident. When the SO-index is negative for a year (May–April), then the dry southeast monsoon in Indonesia and also the southwest monsoon in Central India are usually dryer than normal. In contrast, while the SO-index is still negative, unusual heavy rainfall has begun at San Cristobal in the rainy season preceding the SO-index time period. These teleconnections reach the islands of the equatorial central Pacific a few months later and remain persistent throughout the year. These teleconnection features will become evident again in Section 5. In addition, when the SO-index is negative, the east coast of Africa and Sri Lanka also experience an access of rainfall when the ITCZ moves southward (roughly during October–

December). A corresponding scheme is also developed when the SO-index is positive.

The most important conversion of energy controlling the tropical atmosphere is the release of latent heat. Its influence upon controlling the above mentioned teleconnections (Fig. 3) can be estimated, because areas of large amounts of precipitation are also areas over which large amounts of latent heat are released. Assuming that these areas also have the largest variability in precipitation, then the teleconnections must be strong between tropical rainfall anomalies of these regions. These regions are Bangladesh during the southwest monsoon on the Indian Subcontinent and West Indonesia during the northwest monsoon on the Indonesian Archipelago. In contrast to this assumption, strongest teleconnections have been found over Central India, but cannot be detected over Bangladesh. On the Indonesian Archipelago, teleconnections do occur over West Indonesia, but are strongest over South Indonesia, the driest Indonesian region, during the dry southeast monsoon. These results suggest that the influence of variations of atmospheric latent heating upon teleconnections is small.

5. Composite analysis of the El Niño phenomenon

The composite analysis according to Rasmussen and Carpenter (1982) investigates a time interval of 3 years, in which the defined El Niño-year (January–December) is the centred one. In this study, the following years were defined as El Niño-years because of the positive SST- and rainfall anomalies existing within the equatorial Pacific: 1899, 1905, 1911, 1918, 1925, 1930, 1941, 1951, 1953, 1957, 1965, 1969, 1972 and 1976 (Wooster and Guillan, 1974; Fleer, 1981).

The average rainfall anomalies or composites of selected stations presented in Figs. 5–7 were determined by using the 3-year periods centred over the El Niño years as given at the right top of the figures. A mean SO-index or SO-index

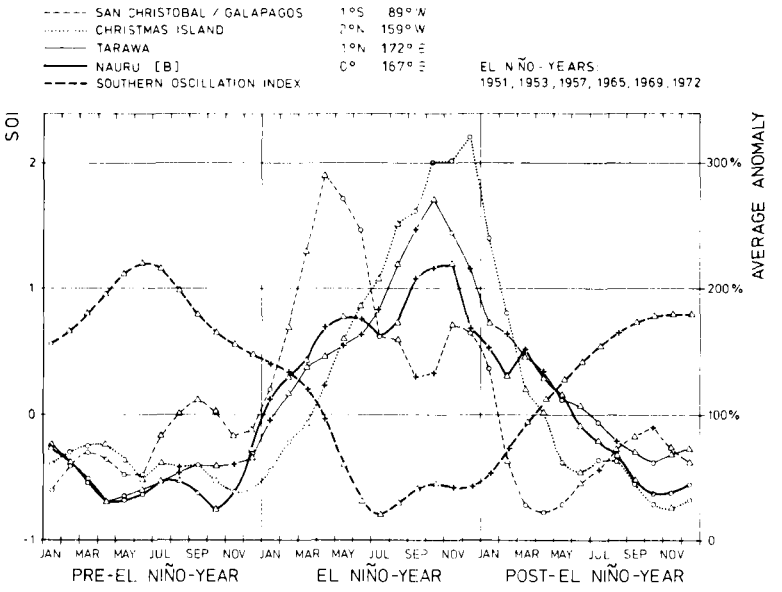

Fig. 5 Composites of San Cristobal, Christmas Island, Tarawa, Nauru, and the SO-index (SOI). The abcissa is the time sequence of a composite, the ordinate the rainfall anomalies in % (on the right) and the SOI (on the left). The signs along the graphs denote the procentual standard deviation (SD) of the corresponding rainfall anomaly:
+: SD ≤ 50%
△: 50% < SD ≤ 100%
○: SD > 100%

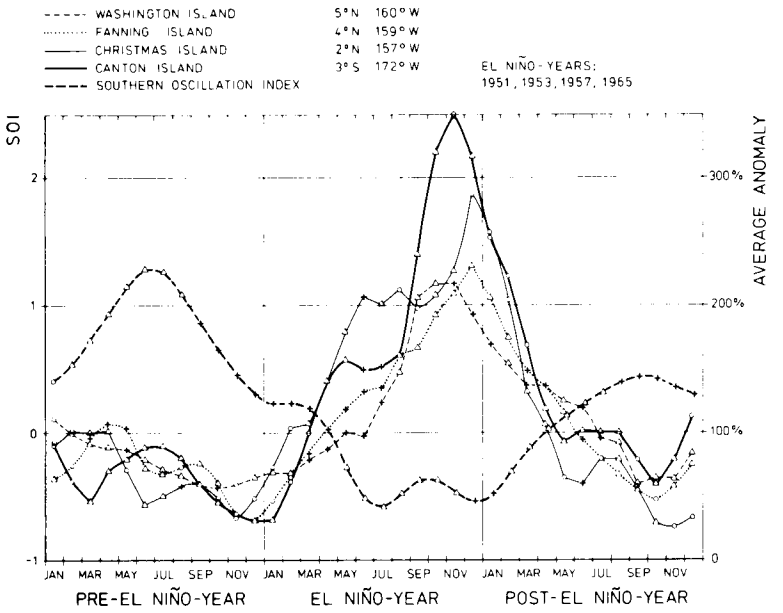

Fig. 6 Composites of Washington-, Fanning-, Christmas-, Canton Island and the SO-index (SOI).

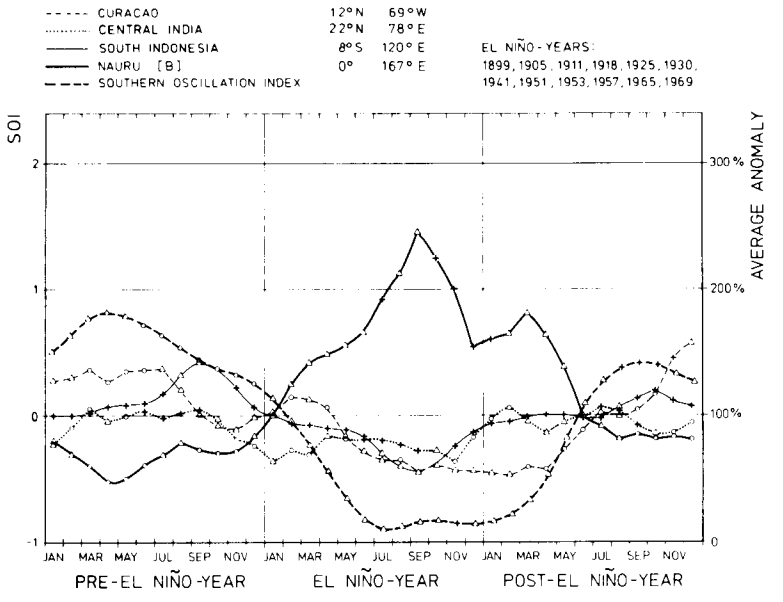

Fig. 7 Composites of Curacao, Central India, South Indonesia, and the SO-index (SOI).

composite during these 3-year periods was determined in the same manner. The standard deviations (in % of the corresponding anomalies) were also determined and are indicated by the different symbols further explained in the legend. As a last step, all composites were smoothed by a 3-month running mean. Figs. 5, 6 show in detail the rainfall anomaly feature over the equatorial

Pacific, whereas Fig. 7 describes rainfall anomalies over the entire region.

Fig. 5 shows the composites of stations zonally along the equatorial Pacific between San Cristobal (89°W) and Nauru (167°E) for the El Niños between 1950 and 1973. The anomalies of 1973 were not available to determine the composites of Nauru and Christmas Island, leading to an inhomogeneity of only little importance for the "Post-El Niño-year". As seen in Fig. 5, in the "Pre-El Niño-year", nearly all anomalies are well below normal. At Nauru and Tarawa, they are below 50% in many months, while the SO-index is positive. During the El Niño-year, the rainfall anomalies start to exceed 100% at Nauru and San Cristobal in January, at Tarawa in February and at Christmas Island in April, and the SO-index becomes negative in April. As early as April, San Cristobal reaches its primary maximum with 290%, while the islands in the Central Pacific experience their maxima of rainfall anomalies between 220% and 320%, half a year later. At this time, San Cristobal experiences its secondary maximum with only 170%. During the Post-El-Niño-year, the anomalies decay rapidly; thus, we observe an east-to-west propagation of the rainfall anomalies along the equatorial Pacific.

In contrast, Fig. 6 shows a spreading of the rainfall anomalies in the meridional direction between Washington Island (5°N) and Canton Island (3°S) along the 160°W circle of longitude for the El Niño-years occurring between 1950 and 1966. The anomaly first exceeding 100% is found in February at Christmas Island, the station closest to the equator, in March at Canton Island, the only station to the south of the equator, in April at Fanning Island and finally in May at Washington Island, the northernmost station. The anomalies of all stations reach their maximum almost simultaneously. The magnitude of rainfall anomalies increases as one moves from the northern stations to the southern stations. Just like the temporal sequence of rainfall anomalies at different stations exceeding 100%, the drop below this value during the northern spring of the Post-El-Niño-year exhibits an identical temporal sequence, starting at stations near the equator and reaching the most poleward stations a few months later.

The composites of Washington-, Fanning- and Christmas Island for the El Niños between 1950 and 1973 (not shown) exhibits the same features as those in Fig. 6. Generally, the occurrence of the maxima of the rainfall anomalies shifts towards the later part of the year and moves from the east to the west as one considers stations east of the dateline, while they occur almost simultaneously all over the equatorial Pacific to the west of it. A similar observation has been made for the SST-anomalies in the same region by Rasmussen and Carpenter (1982).

Thus, from the Figs. 5, 6, we observe that over the Pacific Ocean, rainfall anomalies exceed 100% simultaneously at stations along one circle of latitude, and that this excess first occurs at the equator, and then propagates polewards with a velocity of about 100 km/month.

In order to investigate the large-scale teleconnections observed in Section 4 from a different point of view, we have used the composite analysis for the long rainfall anomaly time series at Curaçao, South Indonesia, Nauru and Central India. The results are plotted in Fig. 7. Also included is the composite of the SO-index for these El Niños (all between 1898 and 1970). The maximum of the negative anomalies at a particular station occurs during the same months when the teleconnections between this particular station with other tropical stations are strongest as shown in Section 4. For example, the largest anomalies occurring in Central India at the end of the southwest monsoon, in South Indonesia in September and at Curaçao during the rainy season, are associated with their strongest teleconnections as shown in Fig. 3. The composites of Nauru and the SO-index are in good agreement with Fig. 5, showing the stability of such composites consisting of only 6 El Niños.

In the time-longitude cross section of Fig. 8, isohyetes of the large-scale rainfall anomalies are displayed based upon several composites along the equator from the east coast of Africa across Indonesia up to Curaçao. All El Niño-events between 1929 and 1970 were considered except for San Cristobal/Galapagos, where only the El Niños between 1950 and 1980 were available. This inhomogeneity of the data base is indicated by the dashed isohyetes. Another inhomogeneity is due to the stations and areas chosen, which do not lie directly on the equator. However, we feel that these inhomogeneities do not significantly influence the results of this analysis.

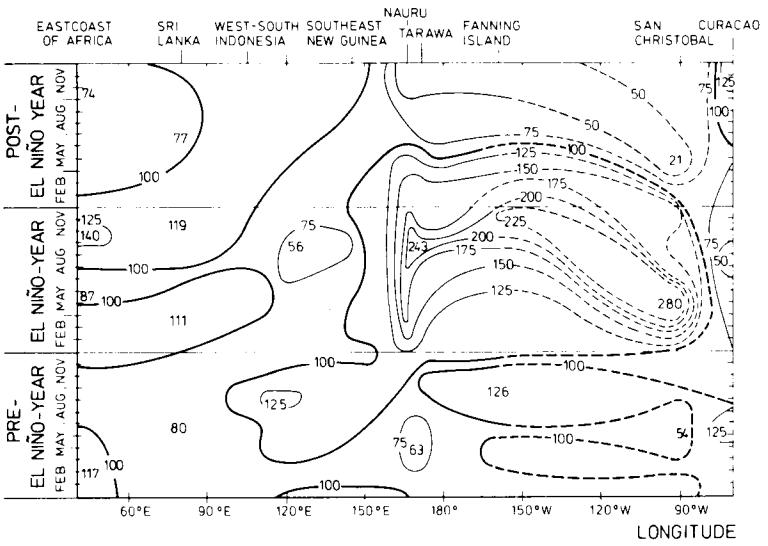

Fig. 8 Time section of composite rainfall anomalies along the equator during an average El Niño. The rainfall anomalies are specified in %. The abcissa is the equator and the ordinate the time sequence.

The pattern displayed in Fig. 8 corresponds to the pattern found in the cross-correlation analysis of Section 4. When rainfall anomalies of Indonesia fall below 100%, the corresponding anomalies of the stations in the equatorial Indian and Pacific Ocean climb above 100%, corresponding to the negative correlations found before. Also, when rainfall anomalies of Indonesia fall below 100%, the corresponding anomalies of Curaçao fall below 100% (positive correlation). During an El Niño-year, the anomalies are largest over the equatorial Pacific. The maximum located at San Cristobal at the beginning of the year shifts westward towards Fanning Island by the end of the year, a feature previously described in Fig. 5. Nearly everywhere, anomalies have extrema during the El Niño-year in the northern fall, the same season as when teleconnections are strongest (see Section 4).

The pattern of Fig. 8 closely corresponds to the pattern of Fig. 22 of Rasmussen and Carpenter (1982), showing a time section of composite SST-anomalies. This suggests that the positive correlation between rainfall anomalies and SST-anomalies over the equatorial central- and eastern Pacific is also present over the eastern Pacific up to Indonesia.

6. Discussion

The scheme of the teleconnections during an El Niño event discovered in Section 4 and mainly confirmed in Section 5 is seasonally fixed and global in scale. These are the positive correlations between the rainfall anomalies of the Indian southwest monsoon, the rainy season at Curaçao, the winter rain of Hawaii and the SO-index on the one side and those of the Indonesian southeast monsoon on the other side, and the negative correlations between the rainfall anomalies within the equatorial Pacific, Sri Lanka during the second intermonsoonal season and the east coast of Africa during the rainy season on the one side and those of Indonesia during the southeast monsoon on the other side. In addition, almost all these regions exhibit teleconnections to one another during these seasons (Section 4). Another interesting feature is the strong persistence of the rainfall anomalies existing at the above-mentioned stations and seasons, whereas the islands of the equatorial central Pacific show a strong persistence lasting for a whole year, starting around June (Section 3).

Some of these teleconnections described in this study have already been discussed in the

literature; however, their strength and seasonal dependence has not yet been investigated. No teleconnections have been previously found for the east coast of Africa, Hawaii and Curaçao, although Meissner (1976) found a negative relation between the winter rain at Hawaii and the rainfall anomalies within the Line Islands. Numerical circulation models have been able to investigate the teleconnections along the equatorial Pacific and of India and Indonesia (e.g. Keshavamurty, 1982), but they were not able to simulate the time lags, and further, most model runs were only computed for a limited special model season.

The mechanisms leading to an El Niño-event are the result of a complicated ocean-atmospheric coupling from which only parts are known. The time lags within the teleconnections recognized in the composite analysis (Fig. 6) give a hint to whether the atmosphere or the ocean is controlling these mechanisms as a primary factor, because the advective time scale of the atmosphere (in the order of days) is much shorter than that of the ocean (in the order of months). Extreme time lags lasting for several months are only present along the equatorial Pacific east of the dateline. The time lag of 8 months between the largest rainfall anomalies at San Cristobal and Christmas Island (Fig. 5) would be consistent with an oceanic current velocity of 0·4 m/s as given by Wyrtki (1981) for the south equatorial current; but this argument cannot be maintained during an El Niño event when this current weakens. Thus, this time lag may be better explained by the propagation of a positive SST-anomaly as described by Kraus and Hanson (1983), which is correlated positively with rainfall anomalies (Bjerknes, 1969).

In contrast to this, it becomes evident in Figs. 5, 6 that rainfall anomalies change their sign simultaneously along the whole Pacific equator when an El Niño event sets in, spreading poleward at a velocity of 100 km/month. This supports the theory of an equatorial Kelvin wave, lowering the thermocline before an El Niño. The spreading poleward of the anomaly can be explained by the switch-off of the equatorial cold water source after the thermocline has been lowered.

The oceanic controlling of the teleconnections east of the dateline also remains sustained by the SST-anomalies during an El Niño exceeding 2 K (Ramage, 1975), while oceanic controlling becomes less important west of the dateline and in the equatorial Indian Ocean where SST-anomalies are well below 1 K. Here, no significant time lags have been discovered (Section 5).

It should be noted that the ocean-atmospheric coupling observed over the Indonesian area (Nicholls, 1981) is also present over the equatorial Pacific (Kraus and Hanson, 1983). This also becomes apparent when comparing Fig. 8 of this paper with Fig. 22 of Rasmussen and Carpenter (1982), because the pattern of rainfall anomalies during an El Niño is almost the same as that of SST-anomalies along the equatorial Indian and Pacific Ocean, confirming the positive correlation between the anomalies of the two.

The slight importance of atmospheric latent heating for the existence of teleconnections has already been discussed in Section 4. The circulation of the southern hemisphere — especially the trade winds — seems to have more influence on the teleconnections. Most of the teleconnections are strongest during the second half of the year and peak in September. This coincides with the seasons when these particular regions are influenced by the southern hemispheric circulation and when this circulation covers the largest area over the globe. Sri Lanka and the east coast of Africa are the exceptions, where the teleconnections are strongest when the ITCZ influences these regions while moving southward.

7. Acknowledgement

This work was performed as part of the author's Diploma thesis at the University of Bonn. Special thanks are due to H. Flohn for remarks and discussions. Financial support was provided by the Max Planck Institut für Meteorologie, Hamburg. W. E. Raatz assisted in preparing this manuscript and M. Lüdecke assisted in drafting.

REFERENCES

Angell, J. K. 1981. Comparison of variations in atmospheric quantities with sea surface temperature variations in the equatorial eastern Pacific. *Mon. Wea. Rev. 109*, 230–243.

Bartels, J. 1935. On the morphology of geophysical time series (in German). *Sitz. Ber. Preuss. Akad. Wiss. Berlin, Phys. math. Kl.*, 504–522.

Becker, C. 1982. On the interaction between rainfall in the tropical regions of America and the large-scale circulation (in German). Diploma thesis, Meteor. Inst. of the Univ. Bonn., Available from Meteor. Inst. of Univ. Bonn.

Berlage, H. P. 1957. Fluctuations in the general atmospheric circulation of more than one year, their nature and prognostic value. Roy. Neth. Met. Inst., Mededlingen en Verhandelingen no. 69. Available from Koninklijk Nederlands Meteorologisch Instituut, De Bilt.

Bjerknes, J. 1969. Atmospheric teleconnections from the equatorial Pacific. *Mon. Wea. Rev. 97*, 163–172.

Donguy, J. R. and Henin, C. 1980. Climatic teleconnections in the western south Pacific with the El Niño-phenomenon. *J. Phys. Oceanogr. 10*, 1952–1958.

Fleer, H. 1981. Large-scale tropical rainfall anomalies. Bonner Meteor. Abh. 26. Available from Meteor. Inst. of Univ. Bonn.

Flohn, H. 1984. Tropical rainfall anomalies and climatic change. *Bonner Meteor. Abh. 31*. Available from Meteor. Inst. of Univ. Bonn.

Helbig, M. 1976. Correlation analysis and analysis of power spectra of additional rainfall series in Africa and reduction of the data by area averaging (in German). Diploma thesis. Meteor. Inst. of Univ. Bonn. Available from Meteor. Inst. of Univ. Bonn.

Ichiye, T. and Pettersen, J. R. 1963. The anomalous rainfall of the 1957–58 winter in the equatorial central Pacific arid area. *J. Meteorol. Soc. Japan 41*, 172–182.

Julian, P. R. and Chervin, R. M. 1978. A study of the Southern Oscillation and Walker Circulation phenomenon. *Mon. Wea. Rev. 106*, 1438–1451.

Keshavamurty, R. N. 1982. Response of the atmosphere to sea surface temperature anomalies over the equatorial Pacific and the teleconnections of the Southern Oscillation. *J. Atmos. Sci. 39*, 1241–1259.

Kraus, E. B. and Hanson, H. P. 1983. Air-sea interaction as a propagator of equatorial ocean surface temperature anomalies. *J. Phys. Oceanogr. 13*, 130–138.

Meisner, B. N. 1976. A study of Hawaiian and Line Island rainfall. Rep. UHMET 76-4. Dept. Meteor. University of Hawaii, Honolulu. Available from Hawaiian Inst. of Geophys., Univ. of Hawaii, Honolulu.

Monthly Climatic Data for the World. 1972–1980. National Oceanic and Atmospheric Administration/National Environmental Satellite, Data, and Information Service/National Climatic Data Center, Asheville, N.C.

Nicholls, N. 1981. Air-sea interaction and the possibility of long-range weather prediction in the Indonesian Archipelago. *Mon. Wea. Rev. 109*, 2435–2443.

Quinn, W. H. and Burt, W. V. 1972. Use of the Southern Oscillation in weather prediction. *J. Appl. Meteorol. 9*, 20–28.

Raatz, W. 1977. Spacial correlation and variability of rainfall in Sri Lanka and South India (Nilgiris) (in German). Diploma thesis. Meteor. Inst. of Univ. Bonn. Available from Meteor. Inst. of Univ. Bonn.

Ramage, C. S. 1971. *Monsoon Meteorology*. International Geophysical Series, Vol. 15. Academic Press. New York and London.

Ramage, C. S. 1968. Role of a tropical 'maritime continent' in the atmospheric circulation. *Mon. Wea. Rev. 96*, 365–370.

Ramage, C. S. 1975. Preliminary discussion of the meteorology of the 1972–73 El Niño. *Bull. Amer. Meteorol. Soc. 56*, 234–242.

Rasmussen, E. M. and Carpenter, T. H. 1982. Variations in tropical sea surface temperature and surface wind fields associated with the Southern Oscillation/El Niño. *Mon. Wea. Rev. 110*, 354–384.

Rasmussen, E. M. and Carpenter, T. H. 1983. The relationship between eastern equatorial Pacific sea surface temperatures and rainfall over India and Sri Lanka. *Mon. Wea. Rev. 111*, 517–528.

Schweizer, B. 1978. Area averages of tropical rainfall (in German). Appendix to the Diploma thesis. Meteor. Inst. of Univ. Bonn. Available from Meteor. Inst. of Univ. Bonn.

Taylor, R. C. 1973. An atlas of Pacific island rainfall. Hawaii Inst. Geoph. Data Rep. No. 25, HIG-73-9. Available from Hawaiian Inst. of Geoph., Univ. of Hawaii, Honolulu.

Trenberth, K. E. 1976. Spatial and temporal variations of the Southern Oscillation *Q. J. R. Meteorol. Soc. 102*, 639–653.

Troup, A. J. 1965. The Southern Oscillation. *Q. J. R. Meteoral. Soc. 91*, 490–506.

Wells, N. C. 1979. The effect of a tropical sea surface temperature anomaly in a coupled ocean-atmosphere model. *J. Geophys. Res. 84*, 4985–4997.

Wooster, W. S. and Guillan, O. 1974. Characteristics of El Niño 1972. *J. Mar. Res. 32*, 387–404.

Wright, P. B. 1975. An index of the Southern Oscillation. Climatic Res. Unit, CRU RP 4, Univ. East Anglia, Norwich, England. Available from Univ. East Anglia.

Wright, P. B. 1977. The Southern Oscillation—patterns and mechanisms of the teleconnections and the persistence. Hawaii Inst. Geophys. Rep., HIG-77-13. Available from Hawaii Inst. Geophys., Univ. of Hawaii, Honolulu.

Wright, P. B. 1979. Persistence of rainfall anomalies in the Central Pacific. *Nature 277*, 371–374.

Wyrtki, K 1973. Teleconnections in the equatorial Pacific Ocean. *Science 180*, 66–68.

Wyrtki, K. 1975. El Niño—the dynamic response of the equatorial Pacific Ocean to atmospheric forcing. *J. Phys. Oceanogr. 5*, 572–584.

Wyrtki, K. 1981. An estimate of equatorial upwelling in the Pacific. *J. Phys. Oceanogr. 11*, 1205–1214.